

Calculation of the Color-Matching Functions of Digital Cameras from their Complete Spectral Responsivities

Francisco Martínez-Verdú^a, Jaume Pujol^b & Pascual Capilla^c

*^a Departamento Interuniversitario de Óptica, Universidad de Alicante
Alicante, Spain*

*^b Centro de Desarrollo de Sensores, Instrumentación y Sensores (CD6),
Universidad Politécnica de Cataluña (UPC)*

Terrassa, Barcelona, Spain

*^c Departamento de Óptica, Universidad de Valencia,
Burjassot, Valencia, Spain*

Abstract

From real spectroradiometric data, we propose an algorithm to obtain the color-matching functions of any digital camera, correctly weighted and according to the corresponding white balance, from the relative scaling of their complete (3-D) spectral responsivities. Thanks to this algorithm, it is possible to predict the RGB digital levels of any digital camera in realistic illumination-scene environments –spatially non-uniform illumination field, variable chromaticity and large dynamic range of luminance levels–, opening the possibility to transform any digital camera into a tele-colorimeter. The illumination-scene test was a Macbeth Color Checker Chart under three different light sources (halogen, metal halide and daylight fluorescent lamps), provided by a non-standard light box. The results confirmed that it is possible to predict any RGB digital levels varying exclusively the f-number of the camera zoom lens.

Introduction

We propose an extension of the well-known opto-electronic conversion function (OECF) for digital image capture devices.¹ We shall call the resulting new function "opto-electronic conversion spectral function" (OECSF). This new concept assumes that the spectral normalized digital level (NDL_{λ}), between 0 and 1, is proportional to the spectral exposure H_{λ} in joules (J) –resulting of the spectral radiance $L_{e\lambda}$ of the monochromatic target, the f-number N of the zoom-lens and the photosite integration time t of the electronic shutter–, the spectral quantum efficiency QE_{λ} , in photoelectrons (e⁻)/incident photons, and the inverse of the opto-electronic conversion constant K_{λ} (e⁻/DL) by photon-transfer technique^{2,3}:

$$NDL_{\lambda} = H_{\lambda} \left[\frac{1}{(2^{bits} - 1) hc} \frac{\lambda}{K_{\lambda}} \frac{QE_{\lambda}}{K_{\lambda}} \right] \quad (1)$$

$$NDL_{\lambda} \propto \frac{L_{e\lambda}}{N^2} t \left[\frac{1}{(2^{bits} - 1) hc} \frac{\lambda}{K_{\lambda}} \frac{QE_{\lambda}}{K_{\lambda}} \right]$$

In this case, we may consider the spectral exposure H_{λ} as the energy input, with the freedom to change exclusively or jointly the f-number N and the photosite integration time t , property known as reciprocity law. The rest of variables enclosed in brackets may be considered as the spectral sensitivity $s(\lambda)$ of the digital image capture system. However, two equivalent concepts may be derived from the general concept of spectral sensitivity:

- Spectral responsivity $r_i(\lambda, H)$: the response to spectral stimuli with constant energy

$$r_{\lambda,i} \equiv r_i(\lambda, H) = \frac{\text{response}(NDL_{\lambda})}{\text{constant energy}(H)} \quad (2)$$

$i = R, G, B \text{ channels}$

- Action spectrum $a_i(\lambda, NDL)$: the inverse of the energy of the spectral stimuli which give constant response

$$a_{\lambda,i} \equiv a_i(\lambda, NDL) = \frac{\text{constant response}(NDL)}{\text{energy}(H_{\lambda})} \quad (3)$$

$i = R, G, B \text{ channels}$

Assuming that this radiometric formalism is correct, this means that, if we want to develop linear models to predict the response of digital cameras, it is necessary to test the following linearity condition: the relative scaling of their complete (3-D) spectral responsivities (or action spectra) would be constant when the spectral exposure (or

equivalently, normalized digital level) is varied. Only if this assumption holds, we can solve successfully the spectral characterization of any digital camera and transform it into an absolute tele-colorimeter using a basis transformation between the RGB camera space and CIE-1931 XYZ space.^{4,5} This formalism is a variant of the standard technique^{6,7,8,9} for measuring the spectral sensitivity of a digital image capture device, by which the user records the device response to monochromatic light across the visible spectrum. However, this empirical approach is different from new mathematical approaches using constrained regressions^{5,10,11} or projections onto convex sets¹² from the recordings of the device responses to a number of objects of known surface reflectance (for example a Macbeth Color Checker Chart) under known illumination conditions.

The purpose of this work is to develop a method to obtain the representative color-matching functions \mathbf{T}_{RGB} associated to the real spectral responsivities of any digital camera, which allows to test the linear performance of these color devices to use them like pseudo-colorimetric instruments. This method was performed on real spectroradiometric data and consists of the following stages:

- Measurement and characterization of the opto-electronic conversion spectral functions (OECSF) and the complete spectral responsivities r_{λ_i} .
- Calculation of the color-matching functions \mathbf{T}_{RGB} from the complete spectral responsivities r_{λ_i} . This algorithm will consider the absolute normalization between the spectral responsivities of the three color-channels and the real white balance initially configured following manufacturer specifications (camera menu), and which is never colorimetrically adjusted.
- A real illumination-scene test to predict the RGB digital levels in realistic illumination and color applying a single camera pseudo-tristimulus model.

Spectral Characterization

Experimental Set-Up

Our digital image capture device consisted of a Sony DXC-930P 3CCD-RGB camera connected to a Matrox MVP-AT 850 frame grabber, inserted into a PC unit. Target radiance was varied using the entrance/exit slits of a CVIS Laser Digikröm DK monochromator with constant spectral resolution, assembled to an Osram HQI T 250W/Daylight vapor fluorescent lamp. Among the fixed initial conditions, which might alter the color output, we set the white balance to 5600 K in manual menu-mode (offset value) and configured the gain and the offset of the analog-digital converter (ADC), to ensure minimal influence on color output, according to the manufacturer specifications. With these initial parameters, we ensured that the RGB data were raw, without unknown internal color matrixing. The target radiance L_{λ} was measured by a Photo Research PR-650 tele-spectroradiometer for the 380-

780 nm wavelength range at 10 nm steps, maintaining the photosite integration time at $t = 20$ ms (offset value) with some selected f-numbers N . The spectral exposure H_{λ} averaged in the exposure series (L_{λ} , N , $t = 20$ ms) for each monochromatic image was given by:

$$H_{\lambda} = 514.982310^{-9} \frac{L_{e\lambda}}{N^2} t [J] \quad (4)$$

Dark current/frame subtraction was applied to each monochromatic image and the normalized digital level NDL was obtained averaging on eight statistical windows larger than 64x64 pixels.

Results

The opto-electronic conversion spectral functions (OECSF's), that is, the NDL_{λ} vs. H_{λ} curves for each RGB channel, were fitted mathematically by sigmoid functions, defined by four parameters as follows:

$$NDL_{\lambda_i} = a_{\lambda_i} + \frac{b_{\lambda_i}}{1 + \exp\left(-\frac{H_{\lambda} - c_{\lambda_i}}{d_{\lambda_i}}\right)} \quad (5)$$

As an example, Figure 1 shows the experimental results for $\lambda = 570$ nm in the R and G channels. The B channel was not sensitive for this wavelength, unlike other digital cameras.^{9,10}

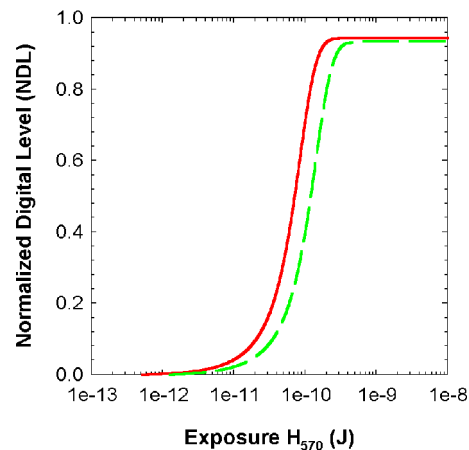


Figure 1. OECSF's measured with $\lambda = 570$ nm, corresponding to the R and G channels of a Sony DXC-930P camera plus a Matrox MVP-AT 850 frame grabber. (Solid line: R channel; dashed line: G channel.)

From these experimental and modelling data, the spectral responsivities $r_{\text{R}}(\lambda, H)$, $r_{\text{G}}(\lambda, H)$, $r_{\text{B}}(\lambda, H)$ and the action spectra $a_{\text{R}}(\lambda, NDL)$, $a_{\text{G}}(\lambda, NDL)$, $a_{\text{B}}(\lambda, NDL)$ are described by:

$$r_i(\lambda, H) = \frac{a_{\lambda_i} + \frac{b_{\lambda_i}}{1 + \exp\left(-\frac{H - c_{\lambda_i}}{d_{\lambda_i}}\right)}}{H} \quad (6)$$

$$a_i(\lambda, NDL) = \frac{NDL}{c_{\lambda_i} - d_{\lambda_i} \ln\left(\frac{b_{\lambda_i}}{NDL - a_{\lambda_i}} - 1\right)}$$

Following with the same example, Figures 2 & 3 show the spectral responsivities and the action spectra of our digital image capture system. It is obvious that the dimensional scale of the spectral responsivities and action spectra is the same due to the opto-electronic conversion spectral function (OECSF) in each wavelength-channel combination. The sudden rise in the responsivity or in action spectrum marks that the spectral exposure (incident photon rate) surpasses the opto-electronic threshold level (dark current/frame photocurrent). The sudden drop in the responsivity (action spectrum) when the digital value approaches its maximum level indicates the saturation of the full optoelectronic wells in both channels. In the middle range, the responsivity (action spectrum) varies smoothly versus spectral exposure (normalized digital level), but never in linear form like a true linear image sensor.

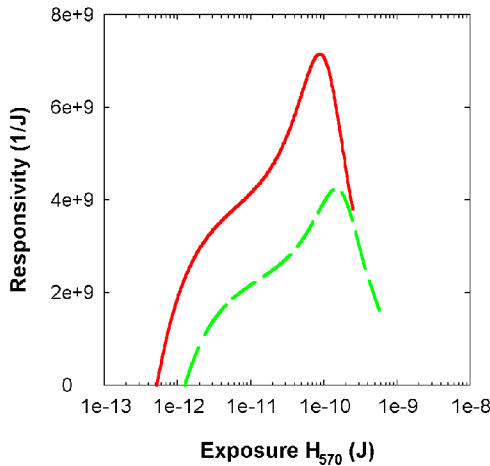


Figure 2. Spectral responsivities of the R and G channels of a Sony DXC-930P plus a Matrox AT-850 measured with $\lambda = 570$ nm. (Solid line: R channel; dashed line: G channel.)

From a global perspective, the above graphs are the 2-dimensional profiles of $r_i(\lambda, H)$ and $a_i(\lambda, NDL)$ 3-D functions (Figure 4). The important question is whether when we select spectral profiles with some constant exposures (or equivalently, normalized digital levels), the relative scaling of the spectral responsivity (action spectrum) would be constant although the absolute scaling were variable. This supposition is verified as shown in Figure 5 for the R channel.

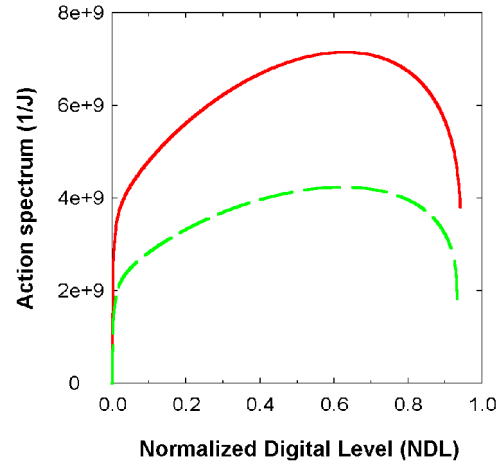


Figure 3. Action spectra of the R and G channels of a Sony DXC-930P plus a Matrox AT-850 measured with $\lambda = 570$ nm. (Solid line: R channel; dashed line: G channel.)

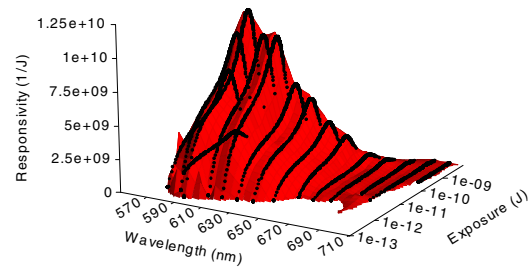


Figure 4. 3-D spectral responsivity of the R channel of a Sony DXC-930P plus a Matrox AT-850. The solid lines are the spectral profiles of the responsivity at variable exposure and fixed wavelength.

Colorimetric Characterization

Proposed Camera Formula

From this radiometric formalism, a new digital pseudo-tristimulus value formula is proposed:

$$DL_i = \left(2^{bits} - 1\right) \sum_{380nm}^{780nm} NDL_{\lambda_i} \Delta\lambda = \left(2^{bits} - 1\right) \sum_{380nm}^{780nm} H_{\lambda} \cdot r_i(\lambda, H) \Delta\lambda \quad (7)$$

Relative Scaling

From these experimental data, the maximum responsivity-peaks were $\lambda_R = 590$ nm, $\lambda_G = 530$ nm and $\lambda_B = 450$ nm. From this camera formula, we obtained the relative scaling of the three spectral responsivities $r_{590R} : r_{530G} : r_{450B} = 1 : 0.6907 : 0.8753$.

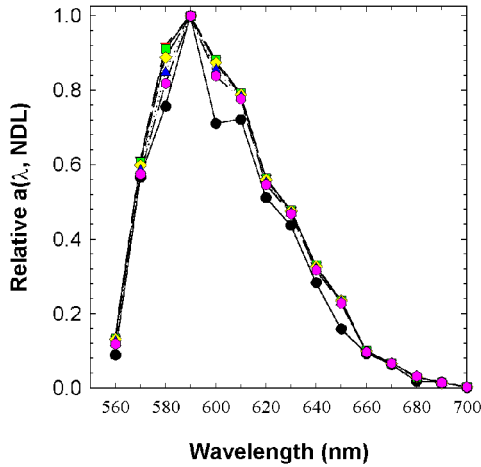


Figure 5. Relative scaling of the action spectrum (spectral responsivity) of the R channel of our digital image capture system. The solid symbols correspond to the following normalized digital levels: 1/255 (threshold, lower solid-line), 10/255, 0.1, 0.2, 0.5 and 0.8.

White Balance Test

With the same camera formula, the real white balance of the camera was tested imposing the equal-energy stimulus $\mathbf{E} = [1, \dots, 1]^t$ with different exposures. The graphic results, shown in Figure 6 and 7, proved that, although the color temperature by camera menu was $T_c = 5600$ K, the colorimetric white balance was 0.8643 : 0.6839 : 1, and not 1:1:1.

Calculation of the Color-Matching Functions

The conversion of the relative RGB spectral responsivities to the color-matching functions \mathbf{T}_{RGB} (41 rows by 3 columns) consisted finally in verifying the equal-energy white balance (Figure 8), so it is possible to compare these color-matching functions with the CIE-1931 XYZ standard observer:

$$\mathbf{T}_{RGB} = [\bar{\mathbf{r}}\bar{\mathbf{g}}\bar{\mathbf{b}}]_{imposing} \mathbf{T}_{RGB}^t \cdot \mathbf{E} \propto \begin{bmatrix} 0.8642 \\ 0.6839 \\ 1 \end{bmatrix}$$

$$with \bar{\mathbf{r}} = \alpha_R \mathbf{r}'_{\lambda R} = \begin{pmatrix} 0.8642 \frac{\mathbf{r}'_{\lambda B} \cdot \mathbf{E}}{\mathbf{r}'_{\lambda R} \cdot \mathbf{E}} \end{pmatrix} \begin{pmatrix} 1 \\ r_{\lambda R} \end{pmatrix} \quad (8)$$

$$with \bar{\mathbf{g}} = \alpha_G \mathbf{r}'_{\lambda G} = \begin{pmatrix} 0.6839 \frac{\mathbf{r}'_{\lambda B} \cdot \mathbf{E}}{\mathbf{r}'_{\lambda G} \cdot \mathbf{E}} \end{pmatrix} \begin{pmatrix} 0.6907 \\ r_{\lambda G} \end{pmatrix}$$

$$with \bar{\mathbf{b}} = \alpha_B \mathbf{r}'_{\lambda B} = (1) \begin{pmatrix} 0.8753 \\ r_{\lambda B} \end{pmatrix}$$

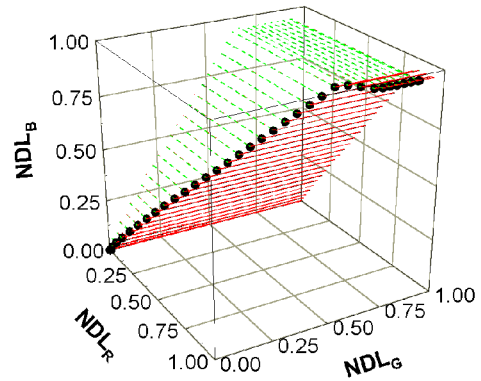
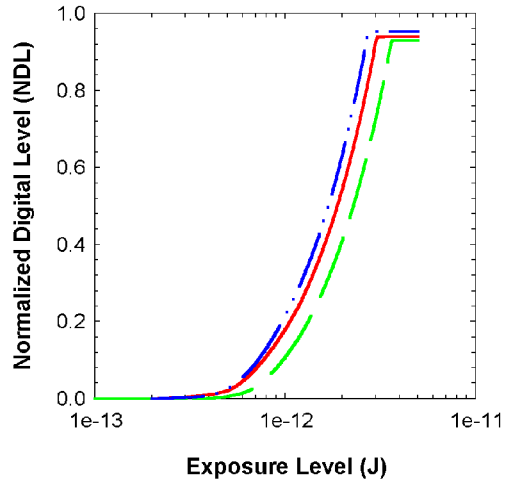


Figure 6 & 7: Colorimetric white balance test for the Sony DXC-930P camera. Above: color responses to equal-energy stimulus with different exposures (Solid line: R channel; dashed line: G channel; dashed-dot-dot line: B channel). Bottom: the inverses of the slopes of the projected lines in R-B and G-B planes are 0.8642 and 0.6839, respectively.

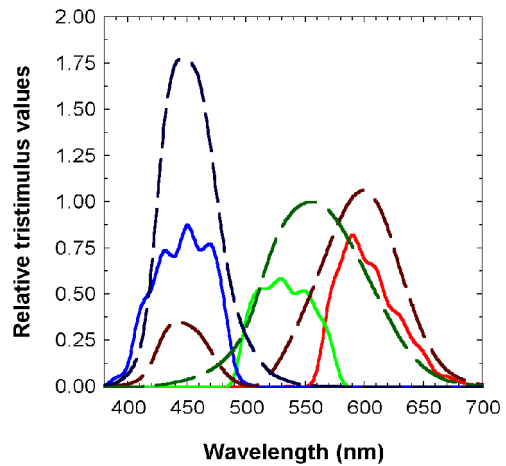


Figure 8: Color-matching functions of the Sony DXC-930P camera (solid lines) compared to the CIE-1931 XYZ standard observer (dashed lines) under the same colorimetric white balance test.

Real Illumination-Scene Test

The purpose of this section is to test a single camera pseudo-tristimulus model recovering the RGB digital levels of the real captures of a scene under different illumination conditions. The real illumination-scene test was a Macbeth Color Checker Chart inside a non-standard light box. A Photo Research PR-650 tele-spectroradiometer and a Halon reference white were used for measuring the real spectral radiances L_{λ} of all the chart patches under three different light sources: INC, halogen lamp; HWL, metal halide lamp; and DAY, daylight fluorescent lamp (Figure 9).

The test consisted in verifying if the RGB digital levels could be recovered imposing one single camera pseudo-tristimulus model using the calculated color-matching functions \mathbf{T}_{RGB} . If $\mathbf{t}_{RGB} = [DL_R, DL_G, DL_B]^t$ are the measured RGB digital levels with subtracting the dark current/frame noises of a set of spectral reflectances \mathbf{p} illuminated under a light source \mathbf{L} (diagonal format), the recovered RGB digital levels \mathbf{t}'_{RGB} can be stated as follows:

$$\mathbf{t}'_{RGB} = \text{noise} + (2^{\text{bits}} - 1) \mathbf{K} \cdot \mathbf{T}_{RGB}^t \cdot (\mathbf{L} \cdot \mathbf{p}) \Delta\lambda$$

$$\text{with noise} = \begin{bmatrix} n_R \\ n_G \\ n_B \end{bmatrix} = \begin{bmatrix} -15.2 \\ -17.7 \\ -11.9 \end{bmatrix} \text{ and } \mathbf{K} = \begin{bmatrix} k_R & 0 & 0 \\ 0 & k_G & 0 \\ 0 & 0 & k_B \end{bmatrix} \quad (9)$$

The f-number N was set to 4 for the INC lamp and 5.6 for the HWL and DAY lamps. Tables 1-3 show the numerical results in absolute RMS RGB error, relative RMS RGB error and average ΔE in CIE-L*a*b* presupposing the RGB digital levels are displayed on an sRGB monitor. These results are also shown graphically in Figure 10. The experimental RGB data due to pixel clipping are included because they are also recovered.

Because the diagonal matrix \mathbf{K} is dependent of the f-number N of the digital image capture device and, possibly, of the spectral sampling $\Delta\lambda$ ($= 10$ nm) that we perform, we think that it is necessary more work about this subject to obtain a complete single digital pseudo-tristimulus model, which covers all the realistic illumination-scene environments (spatially non uniform illumination field, variable chromaticity and large dynamic range of luminance levels) in order to transform a spectracolorimetrically characterized digital camera into an absolute tele-colorimeter.

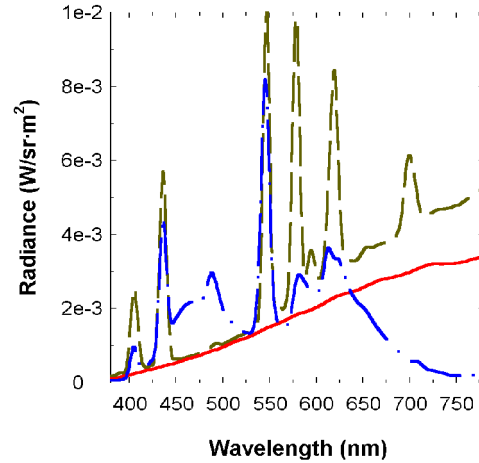


Figure 9: Spectral power distributions of the three light sources using a Halon reference white in the center of the light box and a Photo Research PR-650 tele-spectroradiometer.

Table 1. Numerical results of the predicted data under INC lamp: $k_R = 11.6373$, $k_G = 13.0125$, $k_B = 12.1864$.

	Mean	Max	Min
log (absolute RGB error)	0.93	1.23	0.60
log (relative RGB error)	1.07	1.81	0.33
ΔE (CIE-L*a*b*)	4.65	14.12	1.73

Table 2. Numerical results of the predicted data under HWL lamp: $k_R = 4.1239$, $k_G = 6.2536$, $k_B = 5.4200$.

	Mean	Max	Min
log (absolute RGB error)	1.43	1.97	0.82
log (relative RGB error)	1.24	1.79	0.33
ΔE (CIE-L*a*b*)	13.32	37.02	3.64

Table 3. Numerical results of the predicted data under DAY lamp: $k_R = 5.9137$, $k_G = 5.4641$, $k_B = 5.8349$.

	Mean	Max	Min
log (absolute RGB error)	1.12	1.34	0.94
log (relative RGB error)	1.13	1.84	0.79
ΔE (CIE-L*a*b*)	9.78	16.79	3.98

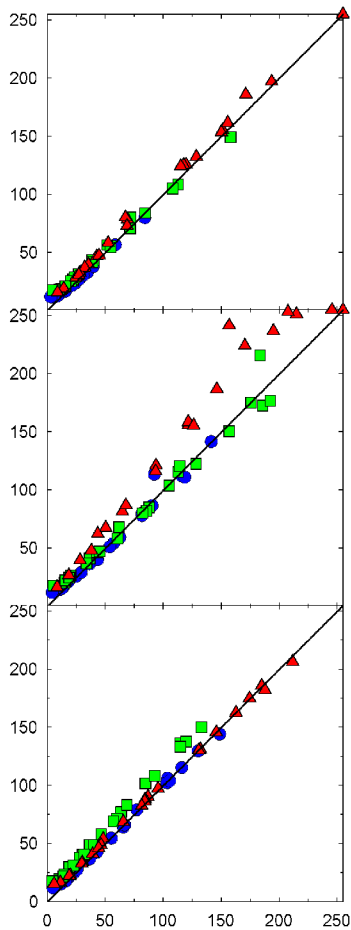


Figure 10: Prediction of the RGB digital levels of the Color Checker Chart under three light sources: top, INC lamp; center, HWL lamp; bottom, DAY lamp. The x-y axes indicate the simulated and experimental data, respectively. (Circles: B channel; squares: G channel; triangles: R channel)

Conclusions

We have presented an experimental and universal spectracolorimetric characterization for any digital still camera using the equivalent terms of spectral responsivity and action spectrum, a new camera formula plus a colorimetric white balance test. We have also proved that any digital still camera is a non-linear color image sensor, because their spectral responsivities, being really 3-dimensional functions, are not constant versus the spectral exposure and normalized digital level. However, the relative scaling of these spectral profiles is approximately the same, so we may consider any digital still camera as a linear color image sensor. Taking into account these considerations, we have also presented an algorithm to

obtain the color-matching functions of any digital image capture device. The resulting color-matching functions have been used to predict the digital RGB levels of a real illumination-scene test using a simple camera pseudo-tristimulus model, which takes into account the background noise, the spectral sampling, the bit depth, and the spectral power distribution of the light source and the spectral reflectance of the object. However, this model is dependent on the relative aperture of the zoom-lens, so more research about this subject is needed to extend this applicability to any luminance dynamic range. Only in this way, we shall be able to transform any digital still camera into an absolute tele-colorimeter.

Acknowledgments

This research was supported by the Comisión Interministerial de Ciencia y Tecnología (CICYT) (Spain) under grants TAP96-0887 and TAP99-0856.

References

1. ISO 14524/DIS, *Method for measuring opto-electronic conversion functions (OECFs)*, ISO/TC42 (Photography) WG18, Geneva, Switzerland (1999).
2. G.C. Holst, *CCD Arrays, cameras and displays*, 2nd Ed., SPIE, Bellingham, WA, 1998.
3. J.R. Janesick, *Charge-Coupled Devices*, SPIE, Bellingham, WA, 2000.
4. G.D. Finlayson and M.S. Drew, *J. Elec. Imaging*, **6**, 484 (1997).
5. ISO 17321, *Color characterization of digital still cameras (DSCs) using color targets and spectral illumination*, WD 4.0, ISO/TC42 (Photography) WG18, ISO/TC130 (Graphic Technology) WG3, Geneva, Switzerland (1999).
6. EBU 3237-E, *Methods of measurement of the colorimetric fidelity of television cameras*, 2nd Ed., Brussels, Belgium (1989).
7. P.M. Hubel, D. Sherman, and J.E. Farrell, A Comparison of Methods of Sensor Spectral Sensitivity Estimation, *Proc. CIC*, pg. 45 (1994).
8. P.L. Vora, J.E. Farrell, J.D. Tietz, and D.H. Brainard, Digital color cameras - 1 - Response models, *HP Technical Report HP-97-53* (1997).
9. P.L. Vora, J.E. Farrell, J.D. Tietz, and D.H. Brainard, Digital color cameras - 2 - Spectral response, *HP Technical Report HP-97-54* (1997).
10. G.D. Finlayson, S. Hordley, and P.M. Hubel, Recovering Device Sensitivities with Quadratic Programming, *Proc. CIC*, pg. 90 (1998).
11. K. Barnard and B. Funt, Camera calibration for color research, *Proc. SPIE*, **3644**, (1999).
12. G. Sharma and H.J. Trussell, Set theoretic estimation in color scanner characterization, *J. Elec. Imaging*, **5**, 479 (1996).